JOURNAL OF Applied Polymer SCIENCE

Modified Poly(vinylidene fluoride) Hollow Fiber Composite Membranes Reinforced by Hydroxyapatite Nanocrystal Whiskers

Wan-Zhong Lang, Qin Ji, Jian-Ping Shen, Ya-Jun Guo, Lian-Feng Chu

The Education Ministry Key Laboratory of Resource Chemistry and Shanghai Key Laboratory of Rare Earth Functional Materials, Shanghai Normal University, Shanghai 200234, People's Republic of China

Correspondence to: W.-Z. Lang (E-mail: wzlang@shnu.edu.cn)

ABSTRACT: The modified poly(vinylidene fluoride) (PVDF) hollow fiber composite membranes reinforced by hydroxyapatite (HAP) nanocrystal whiskers were fabricated with wet-spinning method. The PVDF/HAP/*N*-methyl-2-pyrrolidone dope solutions experienced delayed demixing mechanism, and the precipitation rate slightly increased as the HAP whisker content increased. The cross sections of PVDF-HAP and neat PVDF hollow fiber composite membranes were composed of five distinct layers: two skin layers, two finger-like sublayers, and a sponge-like layer. The Young's modulus of and tensile strength of the PVDF-HAP hollow fiber membranes gradually increased with the addition of nano-HAP whiskers. The elongation ratio was also improved, which was different from the polymeric membranes modified by other inorganic nanofillers. The permeation flux of the PVDF-HAP hollow fiber membranes slightly increased with the increase of HAP content in the composite membranes as its hydrophilicity was improved. The crystallization behaviors of PVDF in the composite membranes were also investigated. © 2012 Wiley Periodicals, Inc. J. Appl. Polym. Sci. 000: 000–000, 2012

KEYWORDS: polyvinylidenefluoride; hollow fiber membrane; composite membrane; hydroxyapatite whisker

Received 13 December 2011; accepted 16 May 2012; published online

DOI: 10.1002/app.38066

INTRODUCTION

Polymeric membranes have been extensively used in water treatment, chemical process, food industry, and pharmaceutical fields. It occupies the major share of membrane market and application fields for the simple preparation process, low price, and better separation performances. However, polymeric membranes have some deficiencies, for example, low hydrophilicity and poor mechanical strength compared with inorganic membranes.[1] To improve the hydrophicility and antifouling capability, many works were devoted to modify polymeric membranes by versatile methods such as chemical grafting, blending, or coating methods.[1–22] Using inorganic nanofillers to modify polymeric membranes is another promising method and many membrane experts have spent much attention on it in recent years.[8–23] The organic–inorganic composite membranes ordinarily have an improved antifouling capability and permeation performances compared with neat polymeric membranes.[11,14,15,20,23]

Poly(vinylidene fluoride) (PVDF) membrane has a superior thermal, chemical stability, and oxidation resistance. It has been extensively applied in microfiltration and ultrafiltration (UF) for general separation purposes.[1–3,12–18] However, it is easily fouled due to its high hydrophobicity, thus causing the decrease of permeation flux, low work efficiency and high operation cost.[1] Several inorganic nanoparticles such as Al_2O_3, ZrO_2, TiO_2, SiO_2 etc. have been used to modify PVDF membrane via/by blending, sol-gel, self-assembly, and so on.[11–24] Lu et al.[12–14] prepared several modified PVDF composite membranes with nano-Al_2O_3 particles by blending method. The hydrophilicity, permeation flux, and antifouling capability of the modified PVDF composite membranes increased with the addition of Al_2O_3. Yu et al.[15,16] reported several novel PVDF hollow fiber composite membranes modified by TiO_2 and SiO_2 fillers with sol-gel method. The hydrophilicity, porosity, and pore size of the novel PVDF membranes increased as TiO_2 or SiO_2 content increased.[15,16] Recently, Liu et al.[17] fabricated the PVDF membranes modified by nano-γ-Al_2O_3 particles, and the improved performances were obtained as well.

The mechanical properties of the PVDF composite membranes modified by nanofillers are ordinarily influenced with the addition of inorganic fillers. For example, Lu's results showed that the mechanical properties of the PVDF/Al_2O_3 blend membranes were strengthened by introducing different amounts of Al_2O_3.[12–14] The blend membranes containing 2 wt % Al_2O_3 had an improved tensile density and elongate ratio by about 50% compared with the neat PVDF membrane. Yu's investigations showed that the tensile stress of PVDF/SiO_2 and PVDF/TiO_2 blend membranes increased, while the elongation at break

decreased with the addition of inorganic fillers.[15,16] Moreover, Liu's results showed that the PVDF/γ-Al_2O_3 with 2 wt % inorganic particles had similar mechanical properties to the neat PVDF membrane. However, the PVDF/γ-Al_2O_3 blend membranes with other γ-Al_2O_3 contents had lower mechanical strength both in tensile strength and elongation ratio.[17] They claimed that it could be attributed to the competition between the dispersion of alumina particles and the amount of double bonds in the complex solution.[17] The different effects of inorganic nanofillers on the resultant PVDF/inorganic blend membranes may be assigned to the properties of inorganic fillers, its integration with PVDF chains, and the membrane preparation conditions.

Hydroxyapatite (HAP), with the compositions of stoichiometric $Ca_{10}(PO_4)_6(OH)_2$ and Ca/P = 1.67, is widely used in biomedical field, due to its chemical and structural similarity to the mineral portion of bones. It is also used as catalyst support, liquid chromatographic columns, lighting material, powder carrier, chemical sensor, drug delivery agent, and so on.[25] Recently, several researchers used HAP nanowhiskers to prepare reinforced polymer composites including high-density polyethylene (HDPE), polyetheretherketon (PEEK), and so on.[26–29] For example, Roeder et al.[26] prepared a kind of reinforced HDPE composites by introducing HAP whiskers. The results showed that the composites reinforced by HAP whiskers had higher elastic modulus, ultimate tensile strength, and work to failure relative to the composites reinforced by spherical HAP. Converse et al.[27] prepared a reinforced PEEK composite with 0–50 vol % HAP whiskers using a novel processing and compression technique. The PEEK composite reinforced with 10 and 20 vol % HAP whiskers exhibited an ultimate tensile strength of 90 and 75 MPa, respectively.

Besides its excellent mechanical properties, HAP whiskers have abundant hydroxyl groups that can be used to improve the hydrophilicity of PVDF membrane and affect the membrane formation process by blending method. In this research, HAP nanowhiskers were used to modify and reinforce PVDF hollow fiber membranes. The effects of HAP nanowhiskers on the precipitation kinetics, morphology, mechanical properties, and crystallization behaviors of the modified PVDF hollow fiber membranes were investigated.

EXPERIMENTAL

Materials

PVDF (FR904, M_n = 380 000) in powder form was purchased from Shanghai 3F New Material Co. (PR China). *N*-methyl-2-pyrrolidone (NMP) involved as solvent was obtained from Sinopharm Chemical Reagent Shanghai Co. (PR China). Lysozyme (M_w = 14,400) was purchased from Shanghai Bio Life Science & Technology Co. (PR China). Cyclohexane and *i*-propanol were purchased from Aladdin-reagent Co., (PR China). Deionized water was obtained by a RO system. HAP nanowhiskers were self-synthesized by a wet chemical precipitation method,[25,26,30] under atmospheric pressure, with calcium nitrate tetrahydrate ($Ca(NO_3)_2{\cdot}4H_2O$) as calcium source and diammonium phosphate ($(NH_4)_2HPO_4$) as phosphorous source. The HAP nanocrystal whiskers have an approximate diameter and length of 10 nm and 100 nm, respectively. The transmission electron microscopy (TEM) image and X-ray diffraction (XRD) pattern of HAP nanocrystal whiskers are illustrated in Figure 1.

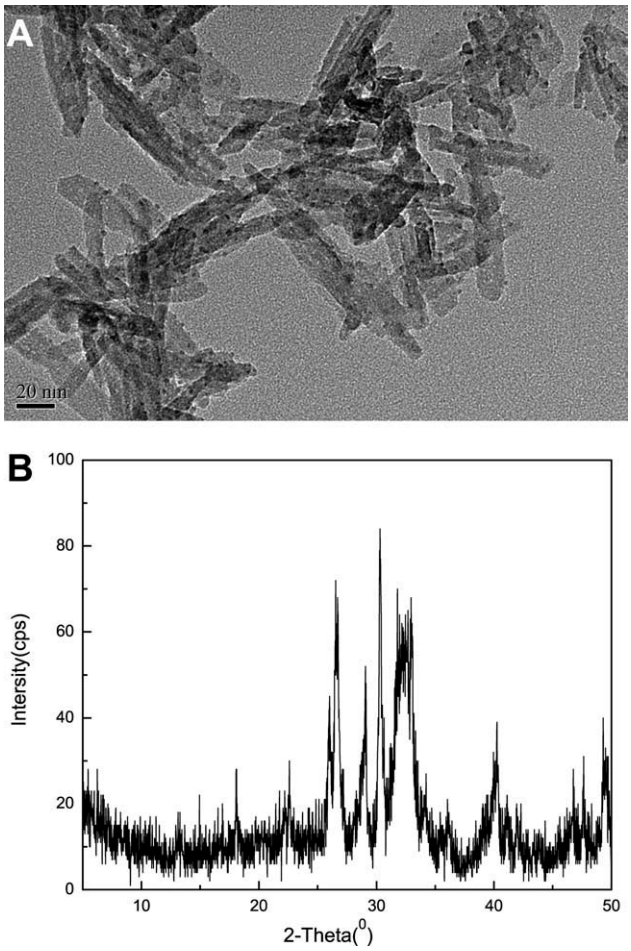

Figure 1. The TEM image (A) and XRD pattern (B) of HAP nanowhiskers.

Light Transmittance Measurement

The precipitation kinetics of PVDF/HAP/NMP dope solutions were measured by a light transmittance experiment. The schematic diagram of device and the detailed experimental procedure have been described in our previous works.[2,3] The cast nascent film was immersed into coagulation bath (deionized water) at 25°C. The transmitted light was detected, amplified, and recorded by a computer system. The intensity of the transmitted light through the cast film was plotted as a function of time.

Preparation of PVDF Hollow Fiber Membranes

PVDF-HAP hollow fiber membranes were spun at 25 ± 1°C with wet-spinning method. The first step was to prepare dope solutions. Four dope solutions containing different HAP contents (0 wt %, 1 wt %, 2 wt %, and 3 wt %), 18 wt % PVDF powder, and solvent NMP were prepared in flask bottles. The mixtures were stirred at 60°C for above 48 h to get uniform dope solutions for spinning. The dope solution was first poured into a feed tank and kept for at least 12 h to degas before

spinning. In spinning process, the dope solution and bore fluid (1.0 mL·min^{-1}) passed through a spinneret with an orifice diameter/inner diameter of the tube of 0.9/0.5 mm at the pressure of N_2 and constant-flow pump, respectively. Deionized water and tap water were used as bore fluid and external coagulation liquid, respectively. The ratio of dope flow rate to bore fluid flow rate was constant in the whole spinning process. The fabricated hollow fiber membranes were stored in deionized water bath for 24 h to remove residual solvent. Then, the spun membranes were kept in 50 wt % glycerol aqueous solution for 24 h to prevent the collapse of porous structure and dried in air at room temperature for testing.

Membrane Characterizations

Morphologies of PVDF-HAP Hollow Fiber Membranes. The morphologies of the prepared PVDF-HAP hollow fiber membranes were examined by a scanning electron microscopy (SEM) (JEOL Model JSM-6380 LV, Japan). The fibers were first immersed into liquid nitrogen for several minutes, then broken and deposited on a copper holder. All samples were coated with gold under vacuum before testing. The external surfaces of the fabricated PVDF-HAP hollow fiber membranes were also measured by an atomic-force microscopy (AFM, BioScope^{TM}) with tapping mode. The mean roughness (R_a) was defined as the average value of the surface relative to the center plane for which the volumes enclosed by the image above and below the plane were equal.

DSC, XRD, FTIR-ATR, Contact Angle, and Mechanical Strength Measurements. The measurements in this section were conducted on dried PVDF-HAP hollow fiber membranes. The method for preparing the dried fibers was described as follows. The wet fibers were successively immersed in absolute isopropanol and absolute cyclohexane liquid for 30 min. Finally, the immersed fibers were taken out and dried in air for the following testing.

The thermal properties of the prepared PVDF-HAP membranes were evaluated by TA instruments (DSCQ100, TA Company). The DSC analyses were carried out under N_2 atmosphere at a heating rate of 10°C min^{-1} from 25 to 300°C. Before DSC measurements, the fibers were thoroughly dried in a convection oven (Keelrein Instrument Co.) at 60°C for 60 min. Subsequently, the fibers were cut to a weight of approximate 0.5 mg piece for testing. XRD patterns of the membranes were recorded on a D/max-r B diffractometer (Rigaku, Japan) equipped with graphite monochromated Cu Kα radiation (λ = 0.15405 nm) operated at 50 mA and 50 kV from 10 to 50°.

FTIR-ATR spectra were collected on a spectrometer Nicolet 380 with a resolution of 4 cm^{-1}, which was conducted on the external surfaces of the fibers.

The contact angles of the external surfaces of the fibers were recorded using the Drop Shape Analyzer (DSA 100, Krüss GmbH, Hamburg, Germany) by sessile-fitting method. The measurement was conducted by dropping 0.5 μL water on the external surfaces of the fibers. The initial contact angles of the samples were adopted.

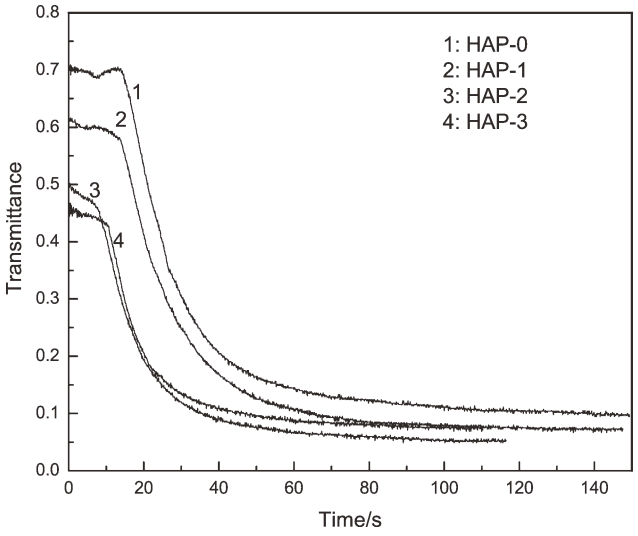

Figure 2. Effects of HAP content on the precipitation kinetics of PVDF/HAP/NMP dope solutions (using deionized water as coagulation fluid at 25°C).

The mechanical properties of the fabricated PVDF-HAP hollow fiber composite membranes were conducted according to Chinese National Standard (GB/T228-2002). It was tested by a material test machine (QJ210A, Shanghai Qingji Instrumentation Sci. & Tech. Co., Shanghai, China). A fiber with 5 cm in length was measured at a loading velocity of 50 mm·min^{-1}. The provided data were obtained by measuring five times for each sample and then averaged.

Permeation Performances of PVDF-HAP Hollow Fiber Membranes. The permeation flux and rejections for lysozyme solute of the membranes were measured by UF experiment. The UF system was self-prepared and described in our previous reports.[2,3] Hollow membrane modules (outside feeding) were 8 mm in diameter. Eight hollow fibers with effective length of 24.5 cm were composed into a module. Lysozyme aqueous solution was applied to UF experiments. The feed concentration was kept at 500 ppm. All experiments were conducted at 25°C with a feed pressure of 1.0 bar. The newly prepared membranes were prepressured at 2.0 bar with deionized water for 1 h before measuring, and then the pure water permeability and rejection of protein solution were tested. The concentrations of permeate and feed solutions were determined by an UV-spectrophotometer (Shimadzu UV-3000, Japan) at the wavelength of 210 nm. Permeation flux (J_w) and rejection (R) were defined as formula (1) and (2), respectively

$$J_w = \frac{Q}{\Delta P \cdot A} \tag{1}$$

$$R = \left(1 - \frac{C_P}{C_F}\right) \times 100\% \tag{2}$$

where J_w is the membrane permeation flux of pure water (L·m^{-2}·h^{-1}·bar^{-1}); Q is the volumetric flow rate of pure water (L·h^{-1}); ΔP is the transmembrane pressure (bar); and A is the effective membrane area (m^2). R is the rejection for lysozyme

Applied Polymer SCIENCE

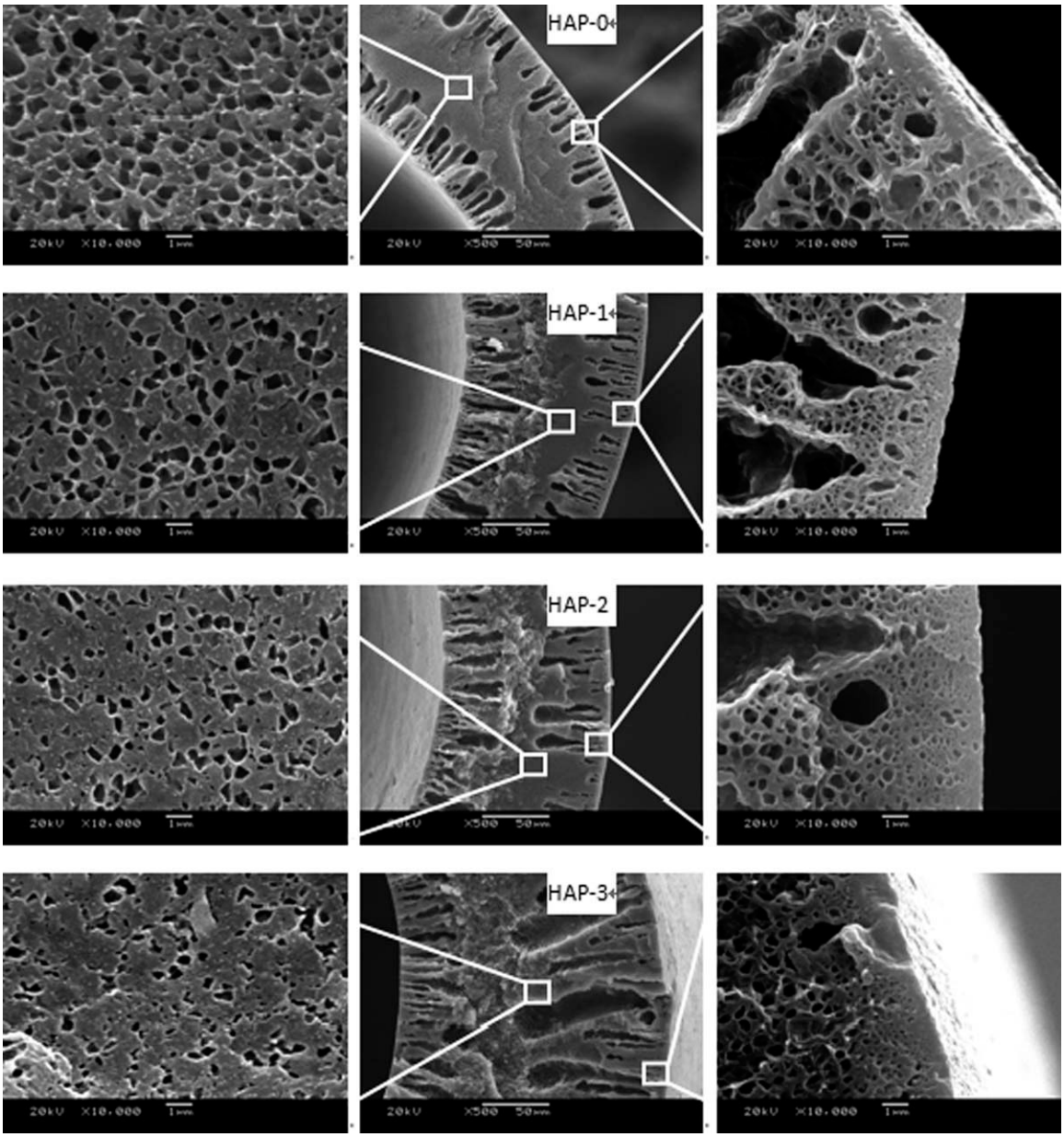

Figure 3. SEM images of the cross sections of PVDF-HAP hollow fiber composite membranes.

protein. C_P and C_F were the concentration of permeate and feed solutions, respectively.

RESULTS AND DISCUSSION

Precipitation Kinetics of PVDF/HAP/NMP Dope Solutions

Light transmittance experiment was applied to measure the precipitation kinetics of four PVDF/HAP/NMP dope solutions with different compositions. Deionized water was used as coagulation bath. The delay time is defined as the time needed before light scattering is induced, detected by a light transmission decrease. According to precipitation rate and delay time, the precipitation process of dope solution in nonsolvent can be divided into instantaneous demixing and delayed demixing.

The precipitation curves of four PVDF/HAP/NMP dope solutions are illustrated in Figure 2. The results showed the four PVDF/HAP/NMP dope solutions generally experienced delayed demixing mechanism. Every precipitation curve can be divided into two stages: delayed demixing stage and quick demixing stage. However, the delayed duration time decreased with the addition of HAP in the dope solutions. It is generally accepted that adding hydrophilic substance in dope solution can accelerate the mutual mass transfer between solvent and nonsolvent and quickens precipitation rate.[31] In this work, the intrinsic hydrophilicity of HAP nanowhiskers promoted the diffusion of nonsolvent to dope solution and accelerated the precipitation rate. Thus, the decreased demixing duration time was observed for the dope solutions containing higher HAP contents. In

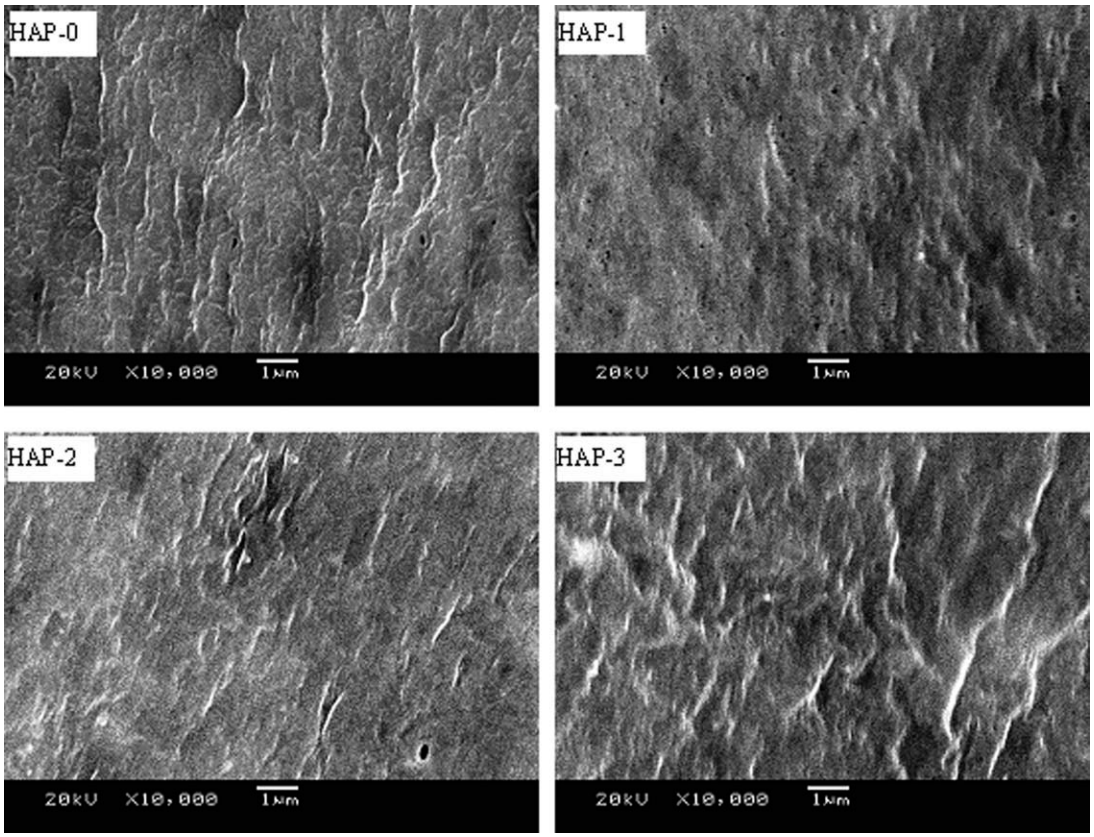

Figure 4. SEM images of the internal surfaces of PVDF-HAP hollow fiber composite membranes.

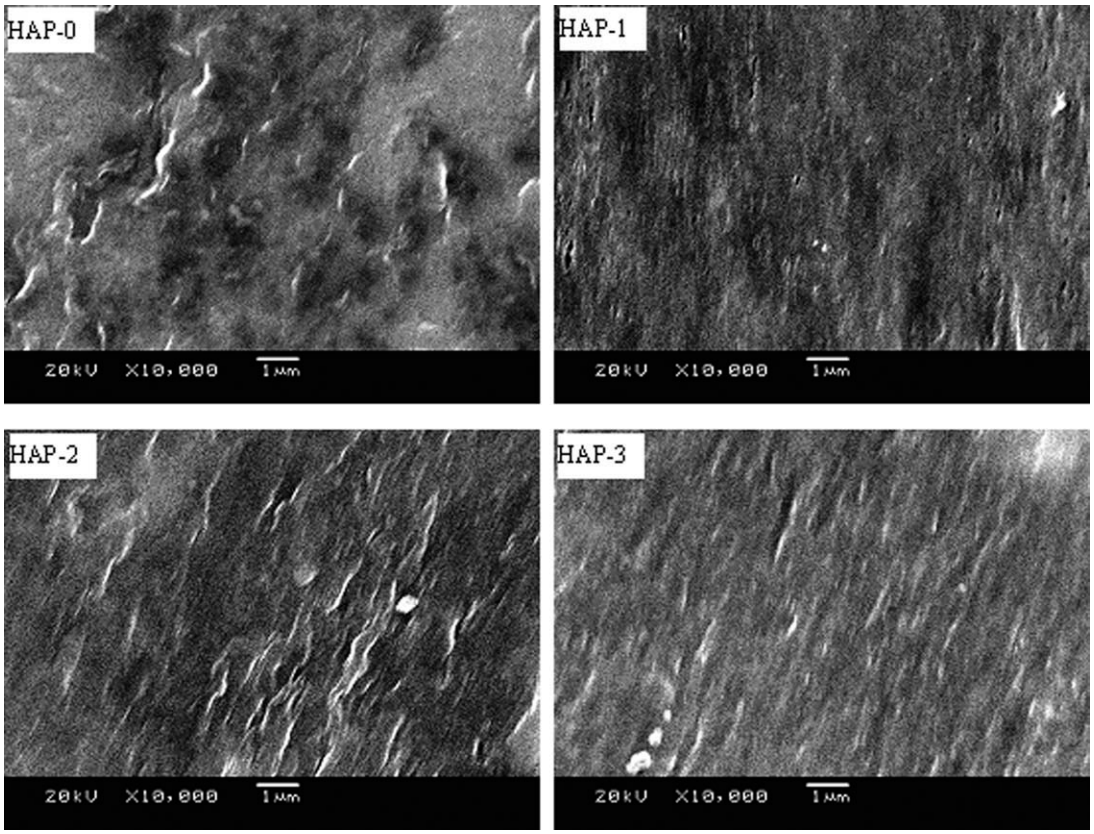

Figure 5. SEM images of the external surfaces of PVDF-HAP hollow fiber composite membranes.

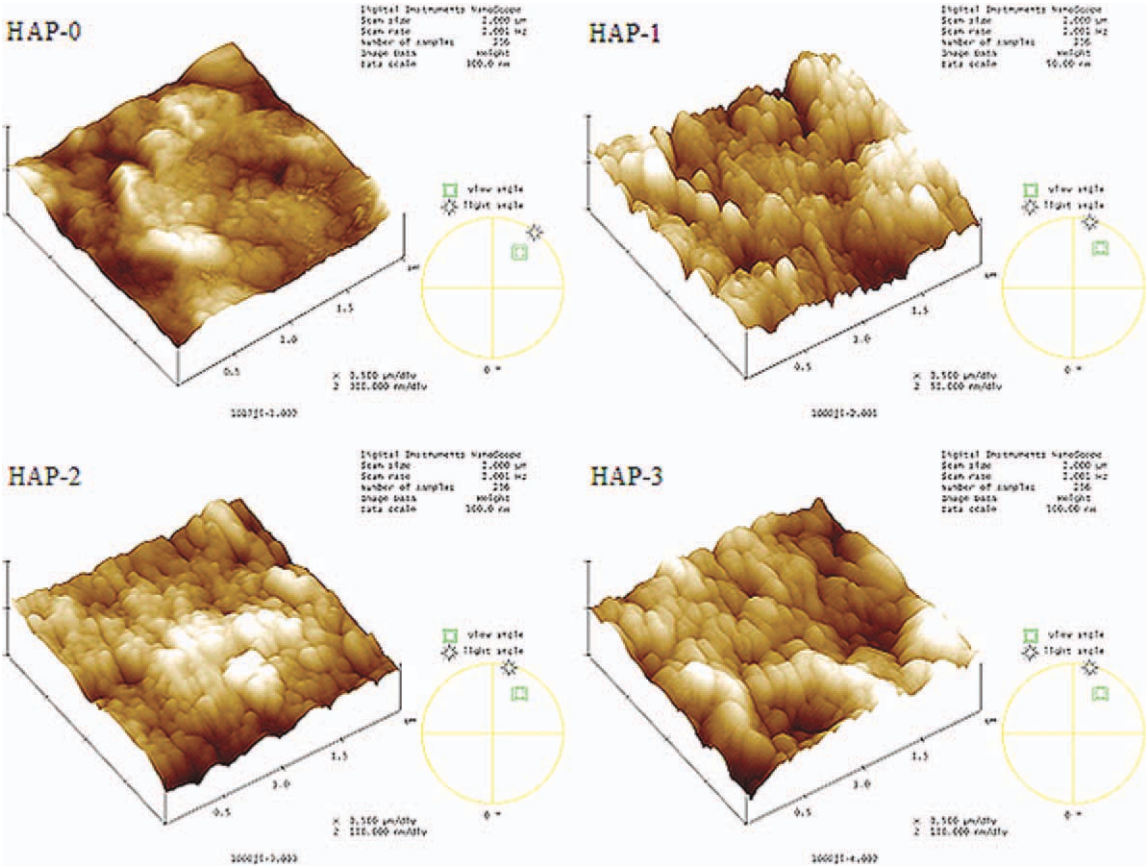

Figure 6. AFM images of the external surfaces of PVDF-HAP hollow fiber composite membranes. [Color figure can be viewed in the online issue, which is available at wileyonlinelibrary.com.]

Figure 2, the initial light transmittance decreased with the addition of HAP whiskers. It can be explained that the nontransparent property of HAP whiskers in the dope solutions caused the decrease of initial light transmittance.

Morphologies of PVDF-HAP Hollow Fiber Composite Membranes

The SEM images of the cross sections, external and internal surfaces of the spun PVDF-HAP, and neat PVDF hollow fiber membranes are shown in Figures 3–5. The cross sections consisted of five distinct layers: two skin layers, double finger-like sublayers beneath the skin layers, and middle sponge-like layer. With the addition of HAP whiskers, the double finger-liker sublayers grew; meanwhile, the middle sponge-like layer sandwiched by the double finger-like sublayers was suppressed. This morphology evolution can be explained on its coagulation process. In Figure 2, the precipitation rate increased as the HAP whisker content increased in the dope solutions, which promoted the development of finger-like structure and thus suppressed the sponge-like sublayers. The local magnified images of the sandwiched sponge-like layers and sublayers are also shown

Table I. The R_a, T_m, and Crystallinity of PVDF-HAP Hollow Fiber Composite Membranes

Membrane no.	R_a (nm)	T_m (°C)	Crystallinity (%)
PVDF powder	/	159.6	28.6
HAP-0	19.088	158.6	36.2
HAP-1	7.270	166.7	37.7
HAP-2	9.064	167.5	37.0
HAP-3	11.670	166.7	36.3

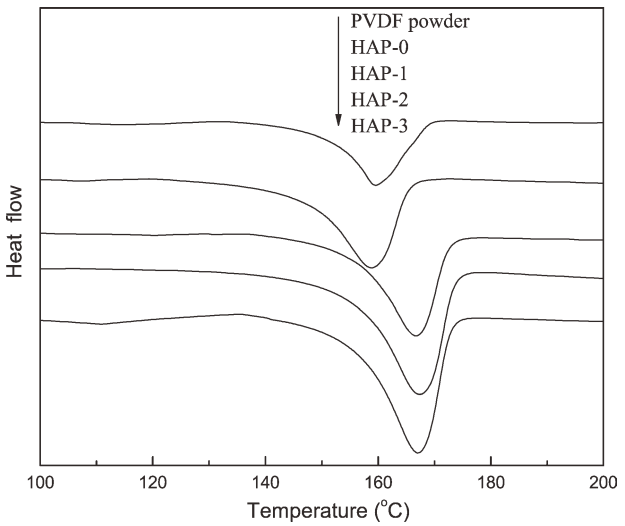

Figure 7. DSC curves of PVDF-HAP hollow fiber composite membranes.

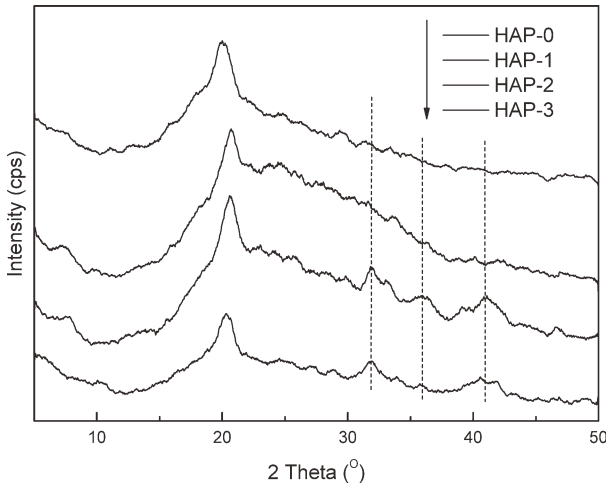

Figure 8. XRD patterns of PVDF-HAP hollow fiber composite membranes.

in Figure 3. It can be seen that the pore number and pore size of the visible pores decreased with the addition of HAP whiskers to the composite membranes. This may be ascribed to the increase of the viscosity of dope solutions with the addition of whiskers, which restricted the development of pores.

Figures 4 and 5 illustrate the morphologies of the internal and external surfaces of the PVDF-HAP hollow fiber membranes, respectively. It can be seen that the dense internal and external surfaces were obtained because the strong nonsolvent (water) was involved as bore fluid and external coagulation liquids.

The external surfaces of the fabricated PVDF-HAP hollow fiber membranes were also measured by AFM technology. The images and the mean surface roughness (R_a) are illustrated in Figure 6 and Table I, respectively. The R_a value first violently decreased from 19.088 nm for HAP-0 to 7.270 nm for HAP-1, and then gradually increased up to 11.670 nm as the HAP content increased from 1 wt % to 3 wt %. As can be seen from Figure 6, the tiny island-like structure was formed on the external surface for HAP-1 sample. Nevertheless, the island size and mean roughness increased with the further increase of HAP content in the composite membranes.

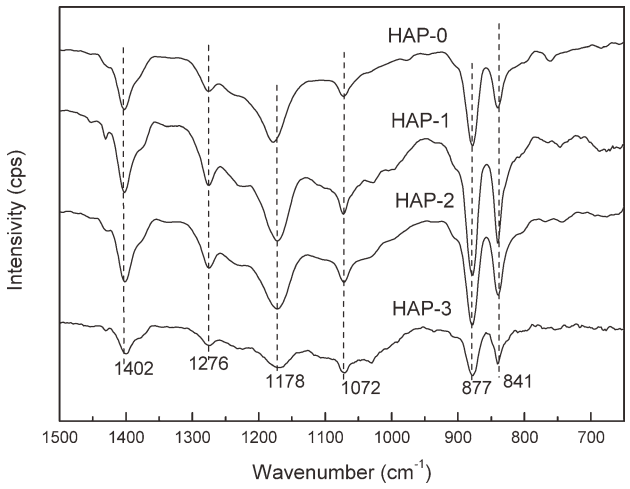

Figure 9. FTIR-ATR spectra of PVDF-HAP hollow fiber composite membranes.

Table II. Mechanical Properties of PVDF-HAP Hollow Fiber Composite Membranes

Membrane no.	Young's modulus (MPa)	Tensile strength (MPa)	Elongation at break (%)
HAP-0	66.76 ± 3.97	2.54 ± 0.07	54.0 ± 6.2
HAP-1	71.22 ± 3.86	3.93 ± 0.26	100.1 ± 7.3
HAP-2	87.95 ± 3.23	3.81 ± 0.05	72.2 ± 12.2
HAP-3	129.93 ± 14.21	4.31 ± 0.11	57.5 ± 5.5

Thermal Properties and Crystallization Behaviors of PVDF-HAP Hollow Fiber Composite Membranes

Figure 7 illustrates the DSC curves of the PVDF-HAP hollow fiber membranes containing different HAP contents. The melting temperature (T_m) values are listed in Table I. It can be seen that T_m of the PVDF-HAP membranes increased with the addition of HAP whiskers. The membrane HAP-0 had a T_m value of 158.6°C slightly below PVDF powder (159.6°C), whereas HAP-1, HAP-2 and HAP-3 membranes had higher, but similar T_m values. The crystallinity values of the membranes were calculated on the ratio of the fusion heat of the samples to that of pure PVDF crystal [140.7 $J{\cdot}g^{-1}$][32] and listed in Table I. It can be seen that the crystallinity slightly increased from 36.2% for HAP-0 to 37.7% for HAP-1 by adding 1 wt % HAP nanowhiskers, and then slowly declined to 36.3% as the HAP content further increased to 3 wt %. The improvement of T_m values and variations of crystallinity of the composite membranes containing HAP whiskers indicated that HAP whiskers had an impact on the rearrangement and crystallization of polymer chains in spinning process.

XRD and FTIR-ATR technologies were conducted to further elucidate the crystallization behaviors of PVDF. Figure 8 illustrates the XRD patterns of the PVDF-HAP hollow fiber membranes containing different HAP contents. In Figure 8, the strongest peaks between 20.1 and 20.9° were observed for the PVDF-HAP composite membranes with different HAP contents, which can be ascribed to the superposition of $\beta(200)$ and $\beta(110)$ reflections.[2,32–36] There were no α phase crystallites in the resultant composite membranes because the peaks below 20° attributed to $\alpha(100)$ and $\alpha(020)$ and the peaks in the range $25 < 2\theta < 30°$ attributed to $\alpha(011)$, $\alpha(120)$, and $\alpha(021)$ were

Table III. Permeation Performances and Contact Angles of PVDF-HAP Hollow Fiber Composite Membranes

Membrane no.	J_w ($L{\cdot}h^{-1}{\cdot}m^{-2}{\cdot}bar^{-1}$)	R (%)	Contact angle (°)
HAP-0	5.9 ± 0.1	95.54 ± 0.12	100.1 ± 3.2
HAP-1	9.6 ± 0.1	90.01 ± 0.42	94.2 ± 2.5
HAP-2	12.1 ± 0.2	92.22 ± 0.03	92.4 ± 3.3
HAP-3	11.1 ± 0.2	95.01 ± 0.09	87.4 ± 1.0

not detected. In addition, the diffraction peaks at 31.9, 35.8, and 41.0° were detected for the composite membranes containing HAP, especially for HAP-2 and HAP-3 membranes, which was in accordance with the characteristic peaks of HAP whiskers shown in Figure 1B. It confirmed the existence of HAP nanowhiskers in the resultant composite membranes.

The FTIR-ATR spectra can further verify the crystalline phase structure of the PVDF-HAP composite membranes (Figure 9). The characteristic peaks of β phase crystallite structure at 841 and 1276 cm^{-1} were seen in each PVDF-HAP composite membrane. Furthermore, the typical bands at 762, 796, 975, 1210, 1383 and 1243 cm^{-1} of α phase crystallites were undetected in the FTIR-ATR spectra.[2,35,37,38] This also confirmed the exclusive existence of β phase crystallites in the resultant PVDF-HAP composite membranes.

Mechanical Properties of PVDF-HAP Hollow Fiber Membranes

Mechanical properties are important for hollow fiber membranes as fiber breaking will let the membranes lose separation performances. The Young's modulus, tensile strength, and elongation at break of the four spun PVDF-HAP hollow fiber composite membranes fibers were determined. The results are shown in Table II. The Young's modulus, tensile strength, and elongation at break of PVDF-HAP hollow fibers were all improved by introducing HAP whiskers. The Young's modulus of PVDF-HAP hollow fiber membranes increased from 66.76 to 129.9 MPa as nano-HAP whisker content increased from 0 to 3 wt %. The tensile strength of the PVDF-HAP composite membranes was evidently improved from 2.54 to 3.81 to 4.31 MPa by adding 1–3 wt % HAP whiskers. However, small difference was observed among the samples of HAP-1, HAP-2, and HAP-3 fibers. The improvement in Young's modulus and tensile strength of PVDF-HAP hollow fiber membranes was similar to the other modified composite membranes by nanofillers.[10,14,15] The elongation at break was also improved by adding HAP nanowhiskers in the PVDF-HAP hollow fiber composite membranes. The elongation at break first increased from 54.0 to 100.1% by adding 1 wt % HAP nanowhiskers, and then declined as the HAP content further increased. These results indicated that adding appropriate amount of HAP nanowhiskers in dope solution can improve the mechanical properties of the resultant membranes. Similar findings have been reported with PVDF membranes blended with Al_2O_3 nanofillers.[12,13] The improved mechanical properties of the synthesized PVDF-HAP hollow fiber membranes in this work may be ascribed to the intrinsic mechanical properties of HAP whiskers. The reinforcement behaviors for polymers with HAP whiskers were also verified in other composite materials.[25–28]

Permeation Performances and Hydrophilicity of PVDF-HAP Hollow Fiber Composite Membranes

Table III shows the permeation performances and contact angles of the PVDF-HAP hollow fiber composite membranes. The pure water permeation flux J_W first increased with the addition of HAP and attained a maximum value when HAP content was 2 wt % and then slightly declined with the further increase of HAP content in the composite membranes. Permeation flux of membrane is generally determined by the membrane morphology and material properties. The hydrophilicity of the PVDF-HAP composite membranes increased due to the contact angles of the external surfaces of the composite membranes varying from 100.1 to 87.4° (Table III) as the HAP content in the dope solutions increased from 0 to 3%. It promoted the improvement of permeation flux from 5.9 $L{\cdot}M^{-2}{\cdot}H^{-1}{\cdot}Bar^{-1}$ for HAP-0 to 12.1 $L{\cdot}M^{-2}{\cdot}H^{-1}{\cdot}Bar^{-1}$ for HAP-2. On the other hand, the permeation flux of the PVDF-HAP composite membranes was also influenced by its morphology. In Figure 3, the pore number and pore size in the sponge-like layers and sublayers evidently decreased as the HAP content increased. It resulted in the slight decline of the permeation flux of HAP-3 compared with HAP-2. In addition, the low porosity of the membranes should account for the generally low permeation flux. The rejections of lysozyme for all PVDF-HAP hollow fiber composite membranes were also measured and listed in Table III. The rejections were all above 90%, which indicated the spun composite membranes owning UF behaviors.

CONCLUSIONS

The modified PVDF hollow fiber composite membranes reinforced by HAP nanocrystal whiskers were fabricated with wet-spinning method. The light transmittance measurement confirmed that PVDF/HAP/NMP dopes experienced delayed demixing mechanism and the precipitation rate slightly increased as the HAP content increased. SEM images showed that a distinct five-layer structure including two skin layers, two finger-like sublayers, and a middle sponge-like layer existed in the cross sections of the fibers. The melting temperature (T_m) increased with the addition of HAP whiskers in the PVDF-HAP composite membranes. Mechanical properties of the PVDF-HAP composite membranes were evidently improved both in Young's modulus and tensile strength. In addition, the elongation at break improved. The permeation flux slightly increased with the addition of HAP in the composite membranes as its hydrophilicity was improved.

The PVDF-HAP composite membranes have improved mechanical properties and can meet long-playing running in water treatment or other separation fields. Introduction of porogens (i.e., polyvinylpyrrolidone and polyethyleneglycol) may enhance the permeation flux of PVDF-HAP composite membranes, which will be investigated in the future.

ACKNOWLEDGMENTS

The research is supported by National Natural Science Foundation of China (Grant No.20906062), Shanghai Municipal Natural Science Foundation (Grant No.09ZR1423300), and Innovation Program of Shanghai Municipal Education Commission (Grant No.12ZZ130).

REFERENCES

1. Liu, F.; Hashim, N. A.; Liu, Y.; Abed, M. R. M.; Li, K. *J. Membr. Sci.* **2011,** *375*, 1.
2. Lang, W.-Z.; Xu, Z.-L.; Yang, H.; Tong, W. J. *Membr. Sci.* **2007,** *288*, 123.

3. Lang, W.-Z.; Guo, Y.-J.; Chu, L.-F. *Polym. Adv. Technol.* **2011,** *22*, 1720.
4. Liu, Z.-M.; Xu, Z.-K.; Wan, L.-S.; Wu, J.; Ulbricht, M. J. *Membr. Sci.* **2005,** *249*, 21.
5. Yi, Z.; Zhu, L.-P.; Xu, Y.-Y.; Zhao, Y.-F.; Ma, X.-T.; Zhu, B.-K. J. *Membr. Sci.* **2010,** *365*, 25.
6. Wavhal, D. S.; Fisher, E. R. *J. Membr Sci.* **2002,** *209*, 255.
7. Wu, D.; Liu, X.; Yu, S.; Liu, M.; Gao, C. J. *Membr. Sci.* **2010,** *352*, 76.
8. Xu, Z.; Wang, J.; Shen, L.; Men, D.; Xu, Y. J. *Membr. Sci.* **2002,** *196*, 221.
9. Li, J.-F.; Xu, Z.-L.; Yang, H.; Yu, L.-Y.; Liu, M. *Appl. Surf. Sci.* **2009,** *255*, 4725.
10. Wu, G.; Gan, S.; Cui, L.; Xu, Y. *Appl. Surf. Sci.* **2008,** *254*, 7080.
11. Yang, Y.; Zhang, H.; Wang, P.; Zheng, Q.; Li, J. J. *Membr. Sci.* **2007,** *288*, 231.
12. Lu, Y.; Yu, S. L.; Chai, B. X. *Polymer* **2005,** *46*, 7701.
13. Lu, Y.; Yu, S. L.; Chai, B. X.; Shun, X. J. *Membr. Sci.* **2006,** *276*, 162.
14. Lu, Y.; Sun, H.; Meng, L. L.; Yu, S. L. *Sep. Purif. Technol.* **2009,** *66*, 347.
15. Yu, L.-Y.; Shen, H.-M.; Xu, Z.-L. J. *Appl. Polym. Sci.* **2009,** *113*, 1763.
16. Yu, L.-Y.; Xu, Z.-L.; Shen, H.-M.; Yang, H. J. *Membr. Sci.* **2009,** *337*, 257.
17. Liu, F.; Moghareh Abed, M. R.; Li, K. J. *Membr. Sci.* **2011,** *366*, 97.
18. Bottino, A.; Capannelli, G.; Comite, A. *Desalination* **2002,** *146*, 35.
19. Kim, D. S.; Park, H. B.; Lee, Y. M.; Park, Y. H.; Rhim, J.-W. J. *Appl. Polym. Sci.* **2004,** *93*, 209.
20. Liu, X.; Peng, Y.; Ji, S. *Desalination* **2008,** *221*, 376.
21. Li, J.-H.; Xu, Y.-Y.; Zhu, L.-P.; Wang, J.-H.; Du, C.-H. J. *Membr. Sci.* **2009,** *326*, 659.
22. Cao, X.; Ma, J.; Shi, X.; Ren, Z. *Appl. Surf. Sci.* **2006,** *253*, 2003.
23. Yu, S.; Zuo, X.; Bao, R.; Xu, X.; Wang, J.; Xu. J. *Polymer* **2009,** *50*, 553.
24. Oh, S. J.; Kim, N.; Lee, Y. T. *J. Membr. Sci.* **2009,** *345*, 13.
25. Zhang, H.; Zhang, M. *Ceram. Inter.* **2011,** *37*, 279.
26. Roeder, R. K.; Sproul, M. M.; Turner, C. H. *J. Biomed. Mater. Res.* **2003,** *67A*, 801.
27. Converse, G. L.; Yue, W.; Roeder, R. K. *Biomaterials* **2007,** *28*, 927.
28. Converse, G. L.; Conrad T. L.; Roeder, R. K. *J. Mech. Behav. Biomed. Mater.* **2009,** *2*, 627.
29. Jiang, L.; Li, Y.; Wang, X.; Zhang, L.; Wen, J.; Gong, M. *Carbohydrate. Polym.* **2008,** *74*, 680.
30. Pan, J.; Lin, K.; Cheng, R.; Chen, Y.; Yu, H. *Tech. Wat. Treat. (Chinese).* **2007,** *33*, 20.
31. Mulder, M. Basic Principles of Membrane Technology; Kluwer Academic Publishers, Enschede, The Netherlands, **1991.**
32. Wang, X.; Zhang, L.; Sun, D. *Desalination* **2009,** *236*, 170.
33. Cheng, L. P. *Macromolecules* **1999,** *32*, 6668.
34. Gregorio, J. R. *J. Appl. Polym. Sci.* **2006,** *100*, 3272.
35. Buonomenna, M. G.; Macchi, P.; Davoli, M.; Drioli, E. *Eur. Polym. J.* **2007,** *43*, 1557.
36. Zhang, M.; Zhang, A. Q.; Zhu, B. K.; Du, C. H.; Xu, Y. Y. *J. Membr. Sci.* **2008,** *319*, 169.
37. Chen, N.; Hong L. *Polymer* **2002,** *43*, 1429.
38. Boccaccio, T.; Bottino, A.; Capannelli, G.; Piaggio P. J. *Membr. Sci.* **2002,** *210*, 315.